

CONFERENCE

INTERNATIONAL



International Conference

250TH

ANNIVERSARY
OF THE 1755
LISBON
EARTHQUAKE

1 to 4 November 2005 · Lisbon · Portugal

TABLE OF CONTENTS**Special Lecture**

- The Lisbon Earthquake of 1 1755 in Spanish Contemporary Authors
Prof. Agustín Udiá, Alfonso López Arroyo - Spain

Invited Lectures

- The Lisbon earthquake of 1 November 1755 - a historical perspectives approach
Prof. Maria do Rosário Themudo Barata - Univ. of Lisbon, Portugal
- The Great Lisbon Earthquake of 1755 and Aceh 2004. Shook the World - Seismologist's Societal Responsibility.
Prof. Karl Fuchs - Univ. Karlsruhe, Germany
- Seismic Engineering: Contribution and Trends to face future 1755 - events
Prof. T. P. Tassios - Nat. Tech. Uni. Athens, Greece

TOPIC 1**Social-economic impact on communities exposed to earthquakes and tsunamis**

- The Last Mile - Earthquake Risk Mitigation Assistance in Developing Countries (Special Lecture)
Prof. Haresh C. Shah, Stanford University, USA
- A Repeat of the 1755 Earthquake Today: Losses and Economic Impacts (Invited Lecture)
Dr. Muir Wood - Risk Management Solutions, London, United Kingdom
- In-situ Assessment, Monitoring and Typification af Buildings and Infrastructure
R. Flesch, M. Ralbousky, M. Eusebio, E. Coelho, B. Hoffmeister, R. Veit
- The 1755 Lisbon Earthquake and the Genesis of the Risk Management Concept
A.Betânia de Almeida
- Vulnerability and Resilience in Disaster Knowledge and Response: Lessons from the 1755 Lisbon Earthquake and the 2004 Indian Ocean Tsunami
F. Pedrosa, R. Richards
- Earthquakes and the coming of age of a scientific attitude in Portugal (1755-1791)
Francisco VAZ
- A system indicators for Disaster Risk Management in the Americas
O. D. Cardona

- Seismic risk evaluation for an urban center
M.L. Carreño, O.D. Cardona, A.H. Barbat 90
- "Knowledge & Practice"; Educational Activities for Reduction of Earthquake impact: The Edurisk Project
R. Camassi, R. Azzaro, V. Castelli, F. La Longa, V. Pessina, L. Peruzza 100
- Related keys in disaster management and diminution in social-economic impact on communities vulnerable to earthquakes and tsunami: example of Guadeloupe island a French overseas department
De, M. Lubino-Bissainte 105
- The Economics of Catastrophes: The role of the Public Administration in the Mitigation of Natural Catastrophes Impacts
Carlos Garrido 107
- Evaluation of the risk management performance
M.L. Carreño, O.D. Cardona, A.H. Barbat 111
- Economic Losses for a Current 1755 Seismic Scenario
J. A. Peláez, A. Delgado García, Antón J. C. Lopez Casado 119
- Survey on Tsunami Risk Awareness in Sri Lanka
T. Kurita, A. Nakamura, M. Kodama, S.R.N. Colombage 122
- Localities Abandoned following earthquakes in Italy. A Lesson for Communities rediscovered through virtual Seismic Itineraries: The Case-History of Sicily
R. Azzaro, R. Camassi, M. Cascone, L. Peruzza 130
- Using Seismic Risk Models As a tools for Risk Management
K. Nasserasadi, M. Ghafory-Ashtiani 135
- Protection against Natural Hazards in Switzerland : Vision and Strategy
Corinne Lacave, Members of PLANAT 141
- TOPIC 2**
- Urban planning facing natural hazards, information and warning**
- Displacement based methods to predict earthquake damage at variable geographical scales. (Invited Lecture)
Prof. Michele Calvi, GMagenes, R. Pinto, Italy 147
- Risk Estimates and Risk Mitigation in Megacities (Special Lecture)
Prof. Friedemann Wenzel, Bendimerad F. Stempniewski L, Germany 160

Simulating Earthquake Scenarios Using Finite-fault Model for The Metropolitan Area of Lisbon (MAL) 164

G. Zonno, A. Carvalho, G. Franceschina, A. Akinci, A. Campos Costa, E. Coelho, G. Cultrera, F. Pacor, V. Pessina, M. Cocco

Application of two different vulnerability Methodologies to Assess Seismic Scenarios in Lisbon 172

C. S. Oliveira, F. Mota de Sá, M. A. Ferreira

The Disaster Management Tool - Concepts and First Training Experiences 178

M. Markus, F. Fiedrich, F. Gehbauer, H. Engelmann, J. Leebmann, C. Schweier, E. Steinle

Earthquake Early Warning - Real-time prediction of ground motion from the first seconds of seismic recordings 185

M. Böse, M. Erdik, F. Wenzel

Risk mapping and disaster scenarios development for urban seismo-prone areas of Russia 188

Mark Klyachko, Valery Larionov, Sergey Sutshev

New Media in Realistic Disaster Scenarios 193

H.P. Bähr

Prognostic estimations facing seismic risk levels in Spain in urban nuclei 198

J. Badal, M. Vázquez-Prada, A. González, Z. Zhang

Seismic vulnerability assessment of buildings in the old city centre of Coimbra 206

R. S. Vicente, J.A.R. Mendes da Silva, H. Varum

A new understanding to catastrophe prevention? 214

M. Bostenaru Dan

Seismic Observation In Urban Area (Seismic Network Around Ljubljana, Slovenia) 222

P. Sincic, R. Vidrih

Contribution of the Distant Seismicity to the Seismic Hazard Values in Portugal 229

J. A. Pelaez, C. Lopez Casado, J. Henares

Casualty scenarios based on laserscanning data 234

C. Schweier, M. Markus, E. Steinle, U. Weidner

Obtaining seismic parameters from small earthquakes 241

A. Jiménez, J. M. García, M. D. Romacho

Earthquake Scenarios and Shake-maps based on Ground motion and Macroseismic Information 245

D. Fäh, P. Kästli, S. Steimen

The role of earthquake forecasting in the sociology and logistics of preparedness 251
E. I. Alves

Simplified Quick Estimation System About Distribution of Seismic Intensity and Building Damage for Seismic Risk Management 257
T. Enomoto, T. Kuriyama, T. Yamamoto, M. Navarro, F. Vidal

Generation of automatic seismic risk scenarios in Catalonia (Spain) 265
X. Goula, T. Susagna, J. Irizarry, N. Romeu

Earthquake scenarios in the North-East Italy: how the variability of input affects the damage assessment and sensitivity analysis 268
F. Meroni, A. Bernardini

The Emergency Plan of Provincia di Potenza: the seismic vulnerability map of buildings for the construction of earthquake damage scenarios. A simulation of 1857 Basilicata Earthquake ($M=6.8$) 276
A. Attolico, A. Bixio, S. Pacifico

Seismotectonics and Seismic Hazard of the Canary Islands 284
L. I. González de Vallejo, J. G. Mayordomo, J. M. Insua

City of Bucharest: Seismic hazard and microzonation of site effects 288
D. Lugu, I. Craifaleanu, A. Aldea, S. Demetriu

Land-use Planning Facing Natural Hazards 296
Dana Procházková

TOPIC 3

Propagation and local effects in the seismic destruction

Observed strong ground motions by dense nation-wide seismic network in Japan and corresponding large-scale simulations using the Earth Simulator. (Invited Lecture) 305
Prof. Takashi Furumura - Earthquake Research Institute, University of Tokyo, Japan

Objective Estimates of the Seismic Intensity of the 1755 Lisbon Earthquake 311
D. R. Brillinger, B. A. Bolt

Contribution to the Damage Interpretation during the 1755 Lisbon Earthquake 317
Margarida San-Payo, Carlos S. Oliveira, P. Teves-Costa, I. Moitinho de Almeida

Did Suboceanic Rayleigh Waves Play a Role on the Heavy Destruction Caused by the 1755 Lisbon Earthquake? 322
A. Yuan, A. Rovelli, G. Mele, E. Priolo

Far-Field Effects of the 1755 Lisbon Earthquake in Catalonia, Spain. Influence of Local Geology and Comparison with 20th Century Macroseismic Data 327
A. Roca, J. Fleta, A. Macau, C. Olivera, T. Susagna

Overview of recent damaging, and low magnitude La Placa (Mw~4.8) earthquake on January 29, 2005: context, seismotectonic and implications for seismic risk SE Spain.
B. Benito, R. Capote, P. Murphy, J. M. Gaspar-Escribano, J. J. Martínez-Díaz, M. Tsige, D. Stich, J. García-Mayordomo, M. J. García, E. Jiménez, J. A. Álvarez-Gómez, J. M. Insua-Arévalo, C. Canora

Damage Fields and Site-Effects Investigations on the 1855 Earthquake in Switzerland
S. Fritsche, D. Faeh, D. Giardini

Upper Limits on Earthquake Ground - Motion Amplitudes from Empirical Data and Theoretical Simulations
F. Sabetta

Foundation Differential Settlement Effects on the seismic Resistance of Pombalino Buildings
R. Cardoso, R Bento, M. Lopes

The impact of hydrogeology on the earthquake ground motion in soft soils.
D. Hannich, H. Hoetzel, D. Ehret, M. Bretorean, A. Danchiv, V. Ciugudean

Seismic Analysis of a Heritage Building Compound in The Old Town of Lisbon
L.F. Ramos, P.B. Lourenço

Seismic Microzonation of Bucharest based on non-linear Modelling
D. Ehret, A. Kienzle, D. Hannich, J. Rohn, V. Ciugudean

A geological subsurface-model for Bucharest as basis for linear modeling of site effects
J. Rohn, D. Ehret, A. Kienzle

Site Effects During the Earthquake on July 12, 2004 in Alpine Region
M. Ribicic, R. Vidrih, P. Sincic

Site response using both subduction and volcanic chain earthquakes. The 2001 El Salvador Seismic crisis
C. Lopez Casado, J. A. Pelaez, J. Henares

Numerical investigation of the Seismic Behaviour of structures on soft and liquefiable soils considering the non-linear soil-Foundation-Structure Interaction
Michael Max Buehler, R. Cudmani

Macroseismic effects of the 23 April 1909 earthquake near Benavente (Portugal)
P. Teves-Costa, J. Batlló

The “Praia do Telheiro” landslide: a 1755 Lisbon earthquake triggered slope instability?
F. M. S. F. Marques

332

340

347

351

358

362

369

372

374

381

386

394

399

TOPIC 4

How to build earthquake resistant buildings under environmental geological constraints

Caveats for nonlinear response assessment Shear Wall Structures (Special Lecture) 407
Prof. Polat Gulkan - METU (Middle East Technical University, Ankara, Turkey)

Rapid Probabilistic Assessment of Structural Systems in Earthquake Regions (Invited Lecture) 417
Prof. Amr Elnashai, S. H. Jeong - University of Illinois at Urbana-Champaign, IL USA

A Scenario Based Seismic damage Estimation for Istanbul 424
A. Yakut, S. Kucukcoba

Development of European shaking tables 430
R. T. Severn

A pilot application of Eurocode 8 for the seismic assessment and retrofit of a real building 435
C. Z. Chrysostomou

The Seismic Behaviour of Reinforced concrete Structural walls: Experiments and Modeling 441
P. Kotronis, J. Mazars, H. Nguyen, N. Lle, J.M. Reynouard, P. Bisch, A. Coin

Building performance during recent earthquakes in the Iberian peninsula and surrounding regions 446
P. Murphy Corella

Seismic evaluation and strengthening of timber structures in traditional buildings 451
M. A. Parisi, M. Piazza

Seismic retrofitting of structural elements. An experimental characterization 458
P. Delgado, V. Rodrigues, P. Rocha, M. Santos, A. Arêde, N. Vila Pouca, A. Costa, R. Delgado

Structural Monitoring of the Monastery of Jerónimos 466
D.V. Oliveira, L. F. Ramos, P.B. Lourenço, J. Roque

Dynamic behaviour of a Pombalino quarter 474
M. Monteiro, M. Lopes, R. Bento

Application of a combined base isolation/supplemental damping seismic protection strategy to a public building in Florence 481
S. Sorace, G. Terenzi

European Experimental research using Shaking tables 487
R. T. Severn

| | | | |
|---|-----|---|-----|
| Current Situation in Application of Seismic isolation technologies in Armenia <i>M.G. Melkumyan</i> | 493 | Whodunnit in 1755? New clues from Sumatra, from the seafloor off SW Iberia and from GPS <i>M.-A. Gutscher</i> | 568 |
| A critical review on seismic fragility curves of cylindrical steel tanks <i>Mehran Seyed Razzaghi, Sassan Eshghi</i> | 501 | Evaluation of the 1755 Earthquake Source using Tsunami Modeling <i>M. A. Baptista, J. M. Miranda</i> | 574 |
| Behaviour of Asymmetric Structures subjected to one directional Near field Ground Motions <i>Armin Aziminejad, A. S. Moghadam</i> | 506 | A Finite - Fault Modeling of the 1755 Lisbon Earthquake Sources <i>A. Carvalho, A. Campos Costa, C. Sousa Oliveira</i> | 578 |
| Reliability of seismic analyses for predicting the performance of R/C Frame Buildings <i>Srdjan Jankovic</i> | 511 | The Tagus Valley seismic hazard and the 1755 earthquake: a critical review <i>L.M. Matias, A. Ribeiro, N. Zitellini, J.M. Miranda, M.A. Baptista, P.T. Costa, P. Terrinha, J. Cabral, R.M. Fernandes</i> | 584 |
| Seismic behaviour of slightly reinforced walls <i>P. Bisch, A. Coin</i> | 518 | The 2004 and 2005 Sumatra earthquakes. Implications for the Lisbon earthquake <i>M. Bezzeghoud, J. F. Borges, B. Caldeira</i> | 592 |
| The role of behavior models in the seismic analysis of structures <i>C. Chesi, M. A. Parisi</i> | 523 | How often events such as the 1755 Lisbon Earthquake occur? Holocene marine paleoseismic record revealed by deep water turbidites and debris flow deposits from the SW Iberian Margin <i>E. Gràcia, A. Vizcaíno, R. Pallàs, J. Garcia-Orellana, A. Asioli, S. Diez, C. Escutia, S. Lebreiro, V. Willmott, D. Casas, and J.J. Dañobeitia</i> | 599 |
| PRRSIE, Program for Seismic Risk Reduction of Educational Facilities <i>Jorge Miguel Proen  a, Carlos Sousa Oliveira, Jos   Freire da Silva</i> | 528 | Bathymetric map of the Gulf of Cadiz, NE Atlantic Ocean: The SWIM Multibeam compilation. <i>S. Diez, E. Gr  cia, M.A Gutscher, L. Matias, T. Mulder, P. Terrinha, L. Somoza N. Zitellin, G. de Alerteis, J. P. Henriet, J. J. Danobeitia</i> | 601 |
| Dynamic analysis of a sdof model of a masonry lintel and peers system <i>C. Casapulla, A Maione</i> | 534 | TOPIC 6 Global response to large Earthquakes | |
| Probabilistic Seismic Risk Assessment of Constructions <i>X. Rom  o, P. Delgado, J. Guedes, A. Costa, R. Delgado</i> | 540 | The 2004 Indian Ocean tsunami: field reconnaissance and eyewitness reports (Special Lecture) <i>Prof. Robin Spence and Antonios Pomonis, United Kingdom</i> | 605 |
| Study of ground motions and damage trends in different building types caused by recent low-magnitude earthquakes in SE Spain. Lessons for defining seismic design criteria <i>J. M. Gaspar-Escribano, P. Murphy, B. Benito</i> | 548 | Towards a Global Response to Large Disasters (Invited Lecture) <i>Prof. Charles Scawthorn - University of Kyoto, Japan</i> | 611 |
| Effectiveness of Seismic Isolation for Cable-Stayed Bridges <i>J. Wilson, M. Wesolowsky</i> | 555 | Risk Management of Aftershocks Accompanied by Large Earthquakes <i>Hidemi Ito</i> | 623 |
| Analytical Study of Flexural Retrofitting of Reinforced Concrete Member <i>F. Shalouf, L. Martinelli</i> | 561 | Seismic Vulnerability assessment of Senigallia (AN, Italy), following the earthquake of 1930 <i>Elena Speranza, Mauro Dolce</i> | 625 |
| TOPIC 5 New approaches to the seismogenesis of the 1755 earthquake | | | |
| New approaches to the seismogenesis of the 1755 Lisbon Earthquake (Invited Lecture) <i>N. Zitellini - ISMAR Institute Science Marine, Italy</i> | 567 | | |

| | |
|---|-----|
| Post-tsunami Urban Damage Assessment in Thailand, Using Optical Satellite Imagery and the VIEWS® Field Reconnaissance System <i>B. Adams, S. Ghosh, C. Huyck, R. Eguchi, C. wabnitz, J. Alder</i> | 633 |
| The next 1755 - Myth and reality; Liability and priorities for action <i>J. Azevedo</i> | 640 |
| Lessons learnt and implemented actions after the 2002 Molise-Puglia Earthquake <i>A. Goretti, Di Ppasquale</i> | 646 |
| City of Bucharest. Buildings vulnerability and seismic risk reduchanactions <i>D. Lungu, C. Arion, R. Vacareanu</i> | 653 |
| Response to Nabire Earthquake in Indonesia: Damage Assessment and safety Strategies <i>Herman Parung</i> | 660 |
| Performance of buildings during the December 26, 2003 Bam Earthquake in Iran <i>Mehrtash Motamedi, Kiarash Naserasadi, Mehran Seyed Razzaghi</i> | 665 |
| Planning actions to develop in case of an earthquake in the AML <i>S. Serrano, C. S. Oliveira</i> | 673 |
| Numerical Model for Trans-Oceanic Propagation of The 26th December 2004 Indian Ocean Tsunami <i>A. Santos, S. Koshimura, F. Imamura</i> | 677 |

SPECIAL LECTURE

Structural Monitoring of the Monastery of Jerónimos

D.V. OLIVEIRA¹, L.F. RAMOS¹, P.B. LOURENÇO¹ AND J. ROQUE²

¹*Universidade do Minho, Civil Engineering Department, Guimarães, Portugal*

²*Polytechnic Institute of Bragança, Bragança, Portugal*

ABSTRACT

The paper details two monitoring systems implemented in the main nave of Santa Maria of Belém Church of the Monastery of Jerónimos, in Lisbon. The monitoring systems were installed to better understand the static and dynamic behavior of the structure, aiming at the damage detection and the improvement of seismic resistance of the monument. Preliminary investigations, numerical non-linear analyses and the first dynamic modal identification analyses are described in the paper. Also the preliminary works for the monitoring systems are presented, including the points selected for observation, discussion of the sensors technical characteristics, as well as preliminary inspection and diagnosis. The first results of the dynamic monitoring system are shown and the future developments on the systems are presented, aiming at a full integration of all the adopted techniques.

INTRODUCTION

Architectural heritage is a key issue to modern societies due to both cultural and economical aspects. Besides the historical aspect, tourism and leisure will be a major industry in the 3rd millennium and the existence of a monument or a monumental compound is often a key attraction of cities and countries.

In the process of preservation of ancient masonry structures, damage evaluation and monitoring procedures are particularly attractive, due to the modern context of minimum repair and observational methods, with iterative and step-by-step approaches. High-priority issues related to damage assessment and monitoring are global non-contact inspection techniques, improved sensor technology, data management, diagnostics (decision making and simulation), improved global dynamic (modal) analysis, self-diagnosing / self-healing materials and improved prediction of early degradation.

The present paper aims at several of the referred issues and is focused in the structural observation of a Portuguese monument: the Santa Maria of Belém Church of the Monastery of Jerónimos, in Lisbon. In the main nave of the church two monitoring structural systems were recently installed in order to understand the static and dynamic structural behaviour with the purpose of damage detection and the improvement of seismic resistance of the monument. Preliminary investigations, numerical non-linear analysis and the first dynamic modal identification analysis are described. Also the preliminary works for the monitoring systems are presented, including the selected points for observation, the discussion of the technical characteristics of the sensors, as well as preliminary inspection and diagnosis. The first results of the dynamic monitoring system are shown and the future developments on the two systems are presented.

GENERAL DESCRIPTION OF THE MONUMENT

The Monastery of Jerónimos is, probably, the crown asset of Portuguese architectural heritage dating from the 16th century. The monumental compound has considerable dimensions in plan, more than 300×50 m², and an average height of 20 m (50 m in the towers). The monastery evolves around two courts. The construction resisted well to the earthquake of November 1, 1755. Later, in December 1756, a new earthquake caused the collapse of one column of the church that supported the vaults of the nave, which resulted in the partial ruin of the nave. In this

occasion also the vault of the high choir of the church partially collapsed, see also Lourenço and Mourão (2001).

The Gothic style was lately introduced in Portugal, incorporating a specific national influence. The so-called “Manueline” style (after King D. Manuel I), exhibits a large variety of architectural influences and erudite motives. An interesting aspect appeared in the 16th century, when the traditional three naves churches start to be replaced by a configuration with small differences in height for the naves. Here, the vault springs from one external wall to the other, are supported in slender columns that divide almost imperceptibly the naves. From the traditional art, only the proportions and roof remain, being the concepts of space and structure novel. The fusion of the naves in the present Church, see Figure 1, is more obvious than in other manifestations of spatial Gothic. For this purpose, the arches are no longer visible, the slightly curved vault comprises a set of ribs and the fan columns reduce effectively the free span. Additional information about the church and the vault can be found in Genin (1995) and Genin (2001).

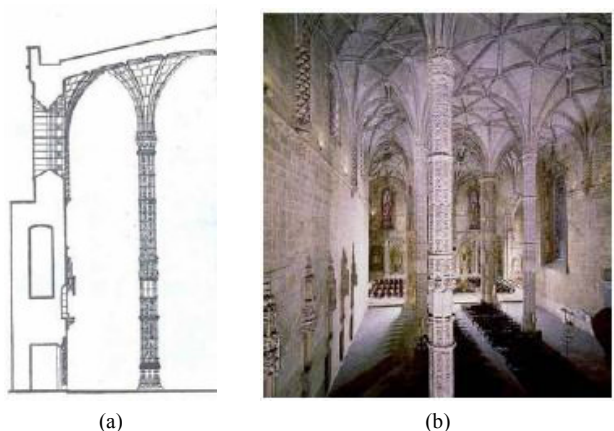


Fig. 1. Church of Monastery of Jerónimos: (a) half of transversal cross-section; (b) aspect of the three naves.

PRELIMINARY INVESTIGATIONS

The problem of safety assessment in historical constructions is quite complex. In particular, little is known about materials and variability of its mechanical properties, existing damage, and constitution of the inner core of the walls, columns and

vaults, among other difficulties. But one key aspect of masonry is its reduced tensile strength, which renders linear elastic analyses debatable. For the purpose of assessing the safety of the Church of Monastery of Jerónimos under vertical loading, two finite element models were developed for the nave and the transept. A preliminary in-situ investigation has also been carried out including geometrical survey, visual inspection, ultrasonic testing and radar testing.

The church has considerable dimensions, namely a length of 70 m, a width of 40 m and a height of 24 m. The plan includes a single bell tower (South side), a single nave, a transept, the chancel and two lateral chapels, see Figure 2. In order to assess the safety of the church, the following preliminary tasks have been carried out: (a) three-dimensional survey of the church; (b) ultrasonic tests in the columns to assess the integrity (Genin, 1995); (c) radar investigation to detect the thickness of the masonry infill in the vault and pier, see Mun (2002) and Oliveira (2002); (d) removal of the roof, visual inspection, bore drilling, metal detection and chemical analysis of materials (Oliveira, 2002).

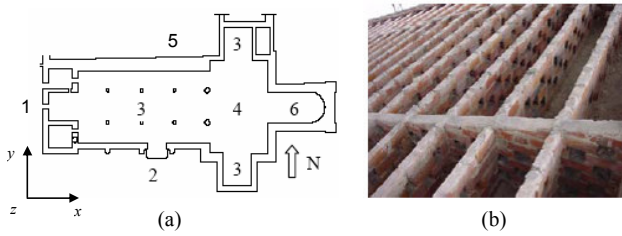


Fig. 2. Survey: (a) Plan, with 1 - Axial doorway, 2 - Lateral doorway, 3 - Nave, 4 - Transept, 5 - Side chapels, 6 - Chancel; (b) removal of the roof and existing system to support the roofing tiles.

The South wall has a thickness of around 1.9 m and possesses very large openings. Three large trapezoidal buttresses ensure the stability of the wall. The North wall is extremely robust (with an average thickness of 3.5 m). This wall includes an internal staircase that provides access to the cloister. The chancel walls are also rather thick (around 2.5-2.65 m).

The nave is divided by two rows of columns, with a free height of about 16.0 m. Each column possesses large bases and fan capitals. The transverse sections of the octagonal columns have a radius of 1.04 m (nave) and 1.88 m (nave-transept). The columns seem to be made of a single block or two blocks, for the nave, and four blocks, for the transept. The topographic survey of the columns presented by Genin (1995) demonstrates the vertical unaligned for all the columns and the external walls, with a maximum of 0.18 m, as it can be observed in Figure 3a.

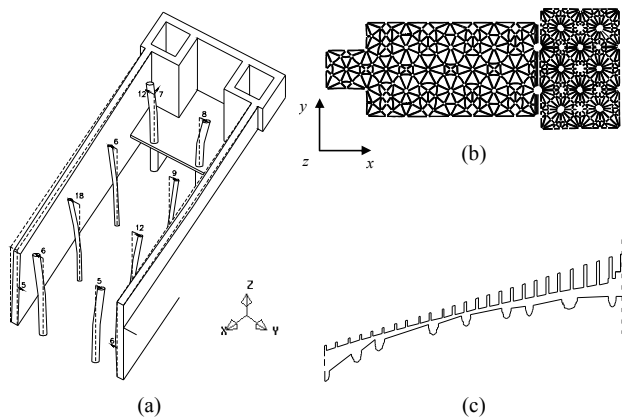


Fig. 3. Aspects of the geometry: (a) topographic survey of the columns and external walls; (b) and (c) plan and transversal cross-section of the nave, respectively.

The vaults are ribbed and are connected to the columns by the large fan capitals, see Figure 3b and Figure 3c. The cross-section of the nave vault is, mostly, a slightly curved barrel vault, even if supported at the columns. Thin stone slabs are placed on top of the stone ribs. On top of the slabs, it exists a variable thickness mortar layer. The part of the slab inside the capital is filled with a concrete-like material with stones and clay mortar. On top of the vaults, brick masonry wallets were built during the 30's to provide support for the roofing tiles, see Oliveira (2002) for details.

NON-LINEAR NUMERICAL ANALYSIS

In ancient constructions, the borderline between architectural details and structural elements is not always clear. The complexity of the structure, addressed in the previous section, increases the difficulty in defining a finite element model appropriate for structural analysis. The lack of historical information and the scarcity of mechanical data limits the quality of the analysis and the interpretation of data. Therefore, the model to be adopted should not be excessively complex.

Analysis of the Main Nave

The adopted model for the main nave includes the structural details representative of the vault, see Figure 4a. Appropriate symmetry boundary conditions have been incorporated. Therefore, the model represents adequately the collapse of the central-South part of the nave. The model includes three-dimensional volume elements, for the ribs and columns, and curved shell elements, for the infill and stones slabs, see Figure 4b.

The external (South) wall was represented by beam elements, properly tied to the volume elements. The supports are fully restrained, being rotations possible given the non-linear material behaviour assumed. All elements have quadratic interpolation, resulting in a mesh with 33335 degrees of freedom.

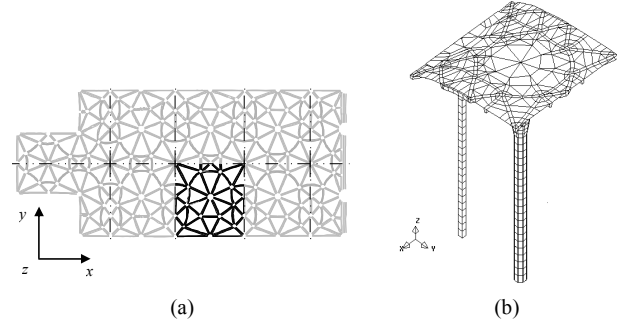


Fig. 4. Aspects of the numerical model: (a) basic pattern; and (b) perspective view of the model.

The actions considered in the analysis include only the self-weight of the structure. Two different types of materials have been considered, one type for the stone masonry plane (Young modulus $E = 3000 \text{ N/mm}^2$ and compressive strength $f_c = 3.0 / \mathbf{6.0} / \text{infinite } \text{N/mm}^2$) and another type for the rubble infill ($E = 1000 \text{ N/mm}^2$ and $f_c = 0.5 / \mathbf{1.0} / 2.0 \text{ N/mm}^2$). Given the uncertainty about the mechanical properties, a sensitive analysis was carried out, assuming the bold values as the reference values. The tensile strength has been assumed equal to zero for both materials. The material model adopted in the analysis was a total strain crack model with an ideal plastic compression limiter, please consult TNO (2002) for further details.

The results for the reference analysis ($f_{c,stone} = 6.0 \text{ N/mm}^2$ and $f_{c,rubble} = 1.0 \text{ N/mm}^2$) are shown in Figure 5, in terms of load-displacement diagrams and maximum principal strain (equivalent to tensile damage). Further discussion of the results can be found in Lourenço and Krakowiak (2003).

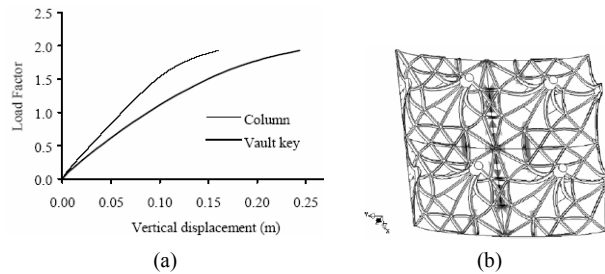


Fig. 5. Results of the nave analysis: (a) load-displacement diagram; (b) maximum principal strains (equivalent to cracks).

Figure 5a illustrates the load-displacement diagrams for the vault key and top of the column. Here, the load factor represents the ratio between the self-weight of the structure and the applied load, meaning that the ultimate load factor is equivalent to the safety factor of the structure. It is possible to observe that the response of the structure is severely non-linear from the beginning of loading, for the nave, and from a load factor of 1.5, for the column. The behaviour of the nave is justified by the rather high tensile stresses found in the ribs, using a linear elastic model. The collapse of the columns is due to the normal and flexural action. The safety factor is 2.0, which is rather low for this type of structures.

The stresses are bounded in tension and compression, meaning that cracking and crushing occurs. Figure 5b illustrates the maximum principal strains, which are related to cracking of the structure. The pairs of transverse ribs that connect the columns (in the central part of the structure) exhibit significant cracking, as well as the infill in the same area. Additional cracking, less exuberant and more diffused, appears in the central octagon defined by the capitals of the four columns. Such cracking occurs at the key of the octagon and in the longitudinal ribs, which confirms the larger displacements of the vault and the bidirectional behaviour of the vault. Finally, the columns exhibit also very high compressive stresses, which lead to the collapse mechanism described before.

The deformed mesh at failure, see Figure 6, indicates that the structural behaviour is similar to a two-dimensional frame, with a collapse mechanism of five hinges (four hinges at the top and base of the columns and one at the key of the vault). Nevertheless, there is some vault effect with slightly larger displacements at the central octagon, formed between the four capitals.

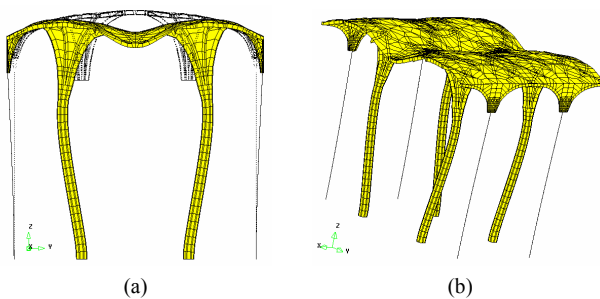


Fig. 6. Deformed mesh failure: (a) cross-section; (b) perspective view.

Further sensibility analyses were developed for different compressive strengths of the stone masonry and infill. From the analyses it was possible to conclude that the influence of the compressive strength of the stone masonry is very significant. The safety factor of the structure is reduced to 1.0, for a compressive strength of 3.0 N/mm^2 , and increased to a value larger than 5.0, for an infinite compressive strength. One the contrary, the influence of the compressive strength of the infill is marginal. The safety factor of the structure is kept constant

and only minor changes of stiffness can be observed. The collapse mechanism remains unchanged in all the analysis.

Analysis of the Transept

The second part of the structural assessment of the church was focused on the transept vault. This vault has a geometry and structural scheme different from the nave. In plan, the vault forms a rectangle with $18.8 \times 28.0 \text{ m}^2$, using a basic square with a side of 4.7 m repeated 24 times. The vault exhibits, in plan, straight and circular ribs, together with keys at the intersection. Given the complexity of the vault and the time consumed in the model of the nave, a simplified two-dimensional model of these arches was adopted for the structural analysis. Figure 7 illustrates the conservative adopted model, which includes the arch, the infill, the nave column and the external wall, with appropriate stiffness values and boundary conditions, see Lourenço and Krakowiak (2003) for a complete description. All elements have quadratic interpolation, resulting in a mesh with 3530 degrees of freedom. Again, the actions considered in the analysis include only the self-weight of the structure. For the materials, the reference values described in the previous section were adopted.

The results for the transept analysis are shown in Figure 7, in terms of maximum principal strain (equivalent to tensile damage) and minimum principal stresses (compression), depicted on the deformed mesh. The safety factor is 1.7, which is again rather low for this type of structures, even if the model is simplified and conservative. Further discussion of the results can be found in Lourenço and Krakowiak (2003).

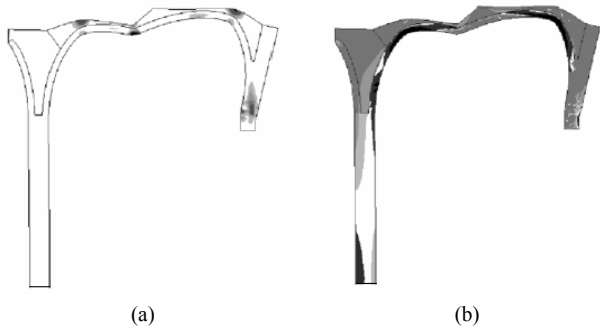


Fig. 7. Results of transept analysis at collapse: (a) maximum principal strains (equivalent to cracks); (b) minimum principal stress (compression), depicted on deformed meshes.

Collapse occurs with a typical four hinges mechanism; being three hinges located in the vault and one hinge located in the right support, see Figure 7. The collapse involving the right wall occurs due to the consideration that the nave prevents inwards movement of the (left) column. Figure 7a indicates that the arch is cracked at the key (intrados) and both quarter spans (extrados). Significant cracking is also present in the right support. Figure 7b demonstrates that high compressive stresses are found in the arch and in the base of the right wall. The compressive stresses in the left column are moderate and do not govern collapse.

DAMAGE DETECTION AND SEISMIC RESISTANCE IMPROVEMENT

In the previous Section the analysis carried out allowed to conclude that: (a) collapse of the nave occurs with a failure mechanism involving the columns and the vault; (b) collapse of the transept occurs with a failure mechanism involving the external walls and the vault; (c) the compressive strength of masonry is a key factor for the response; (d) the safety of the structure seems low, when compared with similar constructions; and (e) the columns of the nave are too slender.

It is stressed that the Church has been in use for some hundred years with moderate damaged ribs, and moderate tilting of the columns and sidewalls. Given the cultural importance of the construction, the safety of the users, the seismic hazard and the accumulation of physical, chemical and mechanical damage, complementary NDT was proposed. Following this idea, an integrated plan of tests and the installation of monitoring systems were proposed, involving the following tasks:

- Characterization of the seismic action in accordance with the location and local foundations of the structure;
- Definition of experimental, in-situ and laboratory tests to better estimate the material properties (modulus of elasticity and compressive strength) of the columns, vaults and rubble material;
- Execution of sonic and radar tests to detect possible damage in the interior of the columns;
- Detailed inspection of the columns and vaults aiming at detecting potentially dangerous aspects in terms of structural safety;
- Execution of other numerical models for the analysis of the entire structure of the nave, to be calibrated by the experimental tests;
- Execution of a dynamic modal identification analysis to calibrate the numerical models and to estimate the modulus of elasticity;
- Installation of two continuous monitoring systems for static and dynamic structural observation, which will help to understand the complex behaviour of the structure and will alert for any unstable deformations or presence of damage.

All the presented tasks are being carried out and they are fundamental for the definition of further actions and for the implementation of a monitoring program. In the following Sections only the last two listed tasks will be discussed.

DYNAMIC MODAL IDENTIFICATION OF THE MAIN NAVE

The first part of the church to be dynamically tested was the main nave where output-only modal identification techniques were used to estimate the modal parameters: resonant frequencies, mode shapes and damping coefficients. These techniques are based on the dynamic response measurements of a virtual system under the natural (ambient or operational) conditions, and they are based on the assumption that the excitations are reasonable random in time and in the physical space of the structure.

Two techniques were applied to compare the estimated dynamic parameters in order to have more accurate results: the Enhanced Frequency Domain Decomposition (EFDD) and the Stochastic Subspace Identification (SSI) method.

The EFDD method derives from the Frequency Domain Decomposition (FDD) method which can be visualized as an extension of the well-known Peak Picking method, see Ewins (2000). In the FDD method, it is assumed that the resonant frequencies are well spaced in frequency domain and the contribution of other modes in the vicinity of that resonant frequencies is null. The method was presented by Brincker et al. (2000) and the main fundament of the method is the Singular Value Decomposition in the frequency domain. The FDD method suffered an improvement, leading to the Enhanced FDD (EFDD) method, see Brincker et al. (2001). Basically the first phase of the EFDD method is equal to FDD but the final estimation of the frequencies values and damping coefficients is calculated in the time domain by the application of the inverse Fast Fourier Transform of each spectral density function for each mode shape.

The SSI method deals directly with time series processing (SSI-DATA, driven stochastic subspace identification), see Rodrigues (2004). This parametric method is robust and allows modal parameter estimation with high precision in frequency

resolution. The counterpart is the fact that the implementation is not as friendly as the FDD or EFDD methods and more processing time is required during the parameter estimation. The method fits a model directly to the raw times series data, based on the state space formulation, directly from the analysis of the response time series. The mathematical model has parameters that can be adjusted to minimize the deviation between the predicted system response and the measured system response.

The EFDD and the SSI methods are implemented in the software ARTeMIS Extractor that was used to process the acquired signals. For the data acquisition, two clock synchronized strong motion recorders with two triaxial force balance accelerometers were used. The measurement equipment is the same as used for the dynamic monitoring system and is presented in detail in the next Section.

According to the results of a preliminary numeric modal analysis with a simplified three-dimensional beam element model, see Figure 8, thirty points on the top of the main nave were selected to measure the acceleration response, see Figure 9a.

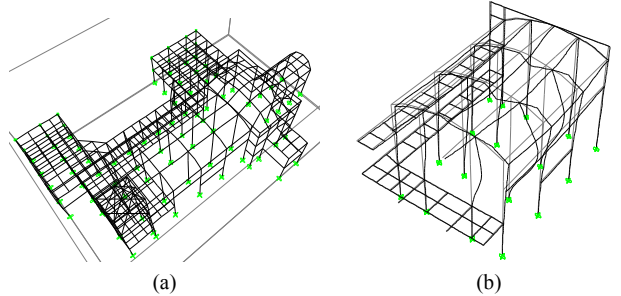


Fig. 8. Aspects of the numerical model: (a) entire element mesh; (b) first mode shape at 1.37 Hz (for the second mode shape a frequency of 1.62 Hz was obtained).

Ten points were localized on the top of the external walls with the purpose of measuring the nave boundaries constrains as well as the global dynamic response of the church. The other points are located either on the top of the columns or on the top of the vaults keys. To assure a good selection of the reference point, preliminary signal measurements were done and it was concluded that point P1 was the one with more significant signal vibration amplitudes. For every measured point, the roof tiles were removed and the signal acquisition was done directly on the top of the nave (extrados) to avoid any possible noise signals from the roof structure, as can be observed in Figure 9b.

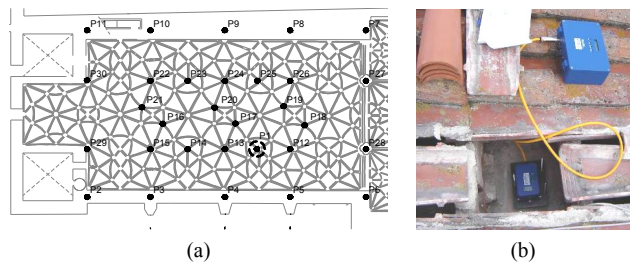


Fig. 9. Measurement points: (a) in-plan location; (b) measurement point in the nave extrados.

The numerical results show that the first expected mode shape was governed by the local effect of the slender columns, see Figure 8b. The first expected frequency was 1.37 Hz and the first ten modes were under 2 Hz, but during the preliminary measurements tests the energy peaks in the spectrums could only be seen between the frequencies values from 3 to 20 Hz. Concerning this information, to estimate that range of frequencies, each data setup was record at 200 Hz (sampling

frequency) with a duration of 10 minutes. The tests were carried out in two days (20 and 21 of April, 2005) at an ambient temperature equal to 18°C, on average.

Table 1 summarizes the eight estimated mode shapes through the two experimental output-only techniques, in terms of resonant frequencies, damping coefficients and Modal Assurance Criteria (MAC). In what concerns the resonant frequencies, the values start from 3.7 to 15.1 Hz and no significant differences could be found between the two methods. The same cannot be concluded for the damping coefficients, where differences up to 140% were observed. The MAC values are discussed later in the paper.

TABLE 1: Measured mode shapes.

| Mode Shape | Frequency [Hz] | | Damping coefficients [%] | | MAC |
|------------|----------------|-------|--------------------------|------|------|
| | EFDD | SSI | EFDD | SSI | |
| Mode 1 | 3.69 | 3.68 | 2.34 | 1.26 | 0.99 |
| Mode 2 | 5.12 | 5.04 | 1.11 | 2.68 | 0.92 |
| Mode 3 | 6.29 | 6.30 | 1.00 | 0.82 | 0.67 |
| Mode 4 | 7.23 | 7.29 | 0.77 | 1.44 | 0.67 |
| Mode 5 | 9.67 | 9.65 | 1.10 | 1.45 | 0.62 |
| Mode 6 | 11.64 | 11.65 | 1.20 | 1.46 | 0.36 |
| Mode 7 | 12.45 | 12.51 | 1.25 | 1.19 | 0.71 |
| Mode 8 | 14.99 | 15.09 | 1.31 | 2.77 | 0.49 |

Figure 10a presents the average of the first three normalized singular values of the spectral density matrix of the EFDD method, where the eight resonant frequencies can be identified. Figure 10b presents the data driven diagram of all data setups for the SSI method. In this case, only the first resonant frequencies are easy to find, but due to the need of a higher state dimension for the models estimation, a huge number of stabilized poles appears, resulting in a more confuse diagram. This fact confirms the difficulty to estimate the higher modes using this method.

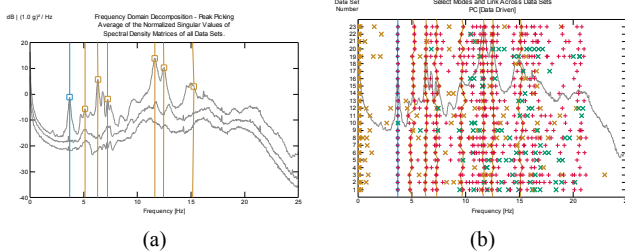


Fig. 10. Estimation diagrams: (a) EFDD method; (b) SSI method.

Figure 11 shows the mode shape configuration for the first two modes. As it was observed in the preliminary numeric analysis, the dynamic response of the main nave is influenced by the dynamic response of the slender columns. The first mode shape is not a global mode of the church, because the nave boundaries do not suffer significant deformations as can be observed in its central part. The mode configurations are essentially composed by components in y (North-South) and z (vertical) directions.

As afore-mentioned, Table 1 presents MAC values calculated for the eight mode shape vectors obtained from two experimental techniques. The MAC criteria are the most well known procedure to study the correlation between two sets of mode shape vectors, see Ewins (2000). The results vary from 0 to 1, i.e. from a bad to a good correlation. Table 1 shows that the two first mode shapes are highly correlated (values closed to the unit), but for the rest of the values it decreases, to a minimum of 0.36. This fact is the result of the difficulties in the

estimation of the mode shapes in the SSI method, as previously discussed.

Nevertheless, this modal identification seems to be acceptable if the structural complexity of the main nave is taken in to account. Even if the mode shape and damping coefficients estimation are not very accurate for the higher modes, the resonant frequencies were accurately calculated by the two experimental techniques for all estimated modes. The next step of this analysis should be the model update in order to validate the numerical model and to calibrate the modulus of elasticity of the material.

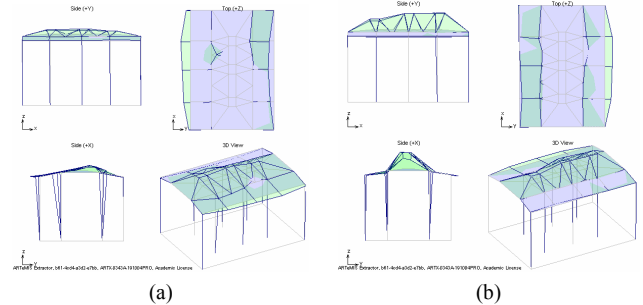


Fig. 11. Experimental mode shape results from EFDD method: (a) first mode shape at 3.7 Hz; (b) second mode shape at 5.1 Hz.

MONITORING SYSTEMS

It is well known that service loads, environmental and accidental actions may cause damage to structures. In this process, long life maintenance plans play an important roll. Regular inspections and condition assessment of engineering structures can allow programming repair works and avoid undesired economic, cultural and life losses. In the case of historical constructions, these aspects are highlighted due to the importance of the structure.

Regarding the results from the preliminary investigations, two monitoring systems were installed in the main nave of the church with the following purposes: (a) to better understand the structural behaviour of the complex construction; (b) to identify any possible progressive phenomenon; (c) to detect damage at an earlier stage; (d) to calibrate the boundary constrains and the elastic modulus required by numerical models; (e) to be useful for future structural strengthening works.

The monitoring systems are long term installations with continuum data records and seasonal reports. In a first phase, narrow time space measurements will be made in order to obtain a first image of the structural behaviour. This time space measurements will gradually increase with the understanding of the structural response. The measurement equipment allows changing the measurements periodicity during service conditions.

The type and location of the sensors and cables was carefully studied in order to minimize the visual impact inside the church, with a close cooperation with the architects from IPPAR, Portuguese Authority for the Architectural Heritage. It is stressed that due to a limited budget, the number of sensors installed in this first phase is reduced, but the monitoring systems are prepared for further sensors upgrading.

Static Monitoring System

The static monitoring system aims at measuring deformations and temperature variations of two columns in the main nave. The measurement system is focused on the columns structural observation, because, as concluded before, these elements control the structural behaviour of the nave.

The static monitoring system is composed by:

- Six temperature sensors (TS1 to TS6), model SKTS 200/U from SKYE INSTRUMENTS, with a measurement range from -20°C to 100°C and a measurement resolution of 0.2°C. Four sensors were installed in the North and South walls and two sensors were installed on the top of the columns and in the nave extrados, see Figure 12 and Figure 13;
- Two uniaxial tilt meters (C1 and C2), model TLT2 from SOIL INSTRUMENTS, with a measurement range of $\pm 1.5^\circ$ and a resolution of 0.03°. The two tilt meters were installed on the top of the columns with larger vertical out-of-plumbness (see Figure 3a) and in the extrados of the nave. The measurement orientation is the transverse direction of the nave (y direction), see Figure 11 and Figure 12;
- One data logger (D) for the data acquisition and data record, model CR10X from CAMPBELL, with a GSM modem from WAVECOM, which allows the data remote downloading by phone line. The data logger is located inside a protection box in the bell tower, see Figure 12 and Figure 13.

In the future, a wind sensor to measure the wind speed and direction and a hygrometer to measure the air moisture will be added to the system, with the purpose of completing the study of environmental influences in the structural behaviour of the church.

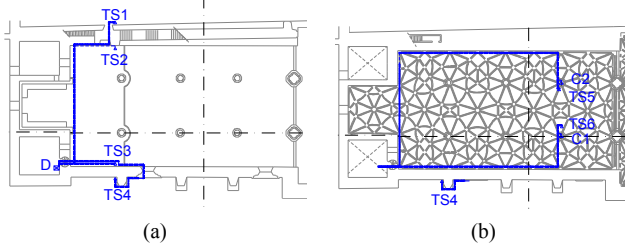


Fig. 12. Static monitoring system: (a) plan of the main nave; (b) plan of the main nave ceiling.

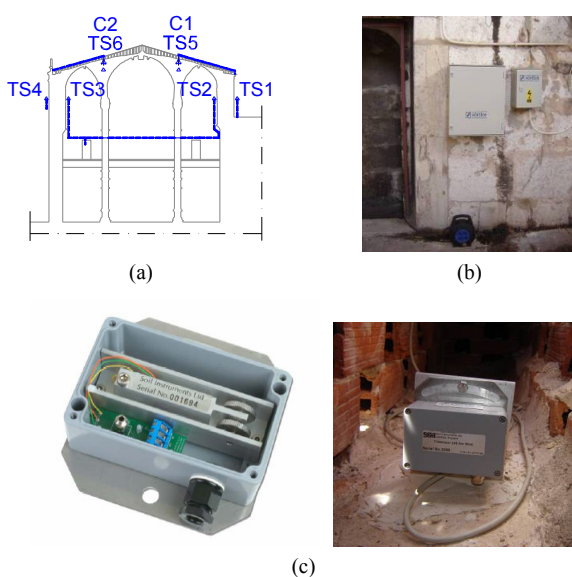


Fig. 13. Static monitoring system: (a) cross-section of the main nave; (b) data logger (c) tilt meter sensor.

It was decided not to include any crackmeter because significant cracks could not be observed in the vaults. However, it is important to proceed with an exhaustive survey to evaluate the state of conservation/deterioration of the vaults joints due to

the fall of mortar and stone pieces from the vault. A brief visual inspection with an elevating platform is being planned to assess the state of conservation of the main nave. After this survey, crack meters can be added to the monitoring system, if necessary.

The sampling rate is 1 sample per hour in order to observe the temperature variation during the one day cycle. The temperature sensors are distributed in the structure to evaluate the effect of the temperature gradient on the response of the structure.

Dynamic Monitoring System

Due to the different technical characteristics and sampling rates of data acquisition, the dynamic monitoring system is physically separated from the static one. The dynamic system is in operation since April 21, 2005. The system is composed by two strong motion recorders; model GSR-18 from GEOSIG; a 18 bits AD converter analyzer. One triaxial force balance accelerometer is connected to each analyzer. The accelerometers, model AC-63 from GEOSIG, have a bandwidth from DC to 100 Hz, a dynamic range $\pm 1\text{ g}$ and a sensitivity of 10 V/g. The two devices connected give a final resolution of 8 μg .

Two points were selected to install the sensors (see Figure 14): one (A1) was installed on the base of the structure near the chancel and the other (A2) on the top of the main nave (extrados), between two consecutive columns and in the locations with higher signal levels in the dynamic modal identification analysis, presented before.

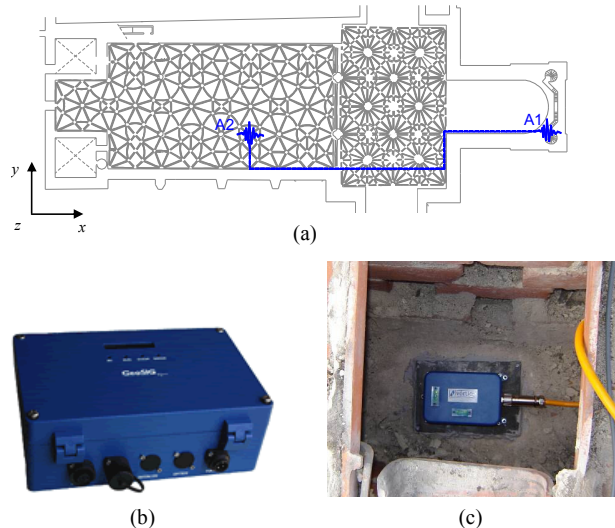


Fig. 14. Dynamic monitoring system: (a) location of the sensors; (b) strong motion recorder; (c) accelerometer on the main nave.

The two recorders are connected by an enhanced interconnection network, which allows a common trigger and time programmed records. Each recorder works independently and the data is stored locally in every recorder. The recorder connected to sensor A1 is the master recorder and enables the synchronization and updates the internal clock of the slave recorder, which, in this case, is the recorder connected to sensor A2. If, in the future, more recorders are added to the system, the same network can be extended to the new apparatus. There is also the possibility to connect the network recorders to a GPS for clock synchronization and to a phone modem for data transfer. This solution was not adopted, because the amount of data information in the data files would be too large for the dynamic tests and the GPS would increase significantly the costs of the system.

It is known, see Doebling et al. (1996), that changes in element dimensions, in the boundary conditions, in the mass distribution and the degradation of the mechanical properties of the materials, including the damage process, or the simultaneously occurrence of all these phenomenon affect the dynamic behaviour of structures, i.e. changes the resonant frequencies, mode shapes and damping coefficients. If the environmental influence (temperature, moisture, etc) is evaluated and separated from the dynamic response of the structure, see Peeters (2000), the damage occurrence can be globally detected and additional plans can be implemented in order to detect and estimate the damage more accurately and, then, evaluate their consequences to the construction.

Due to the fact that damage is, in most cases, a localized phenomenon, the experience of several researchers allowed concluding that damage detection requires not only the observation of the resonant frequencies changes, but also the mode shapes changes and the quantities that can be calculated from their values, especially for the higher modes, see Maeck (2003). The actual number of sensors installed in the church is not enough to monitor its dynamic behaviour by mode shape changes. So, during the first phase and until the first sensor upgrade, the dynamic monitoring system will be processed by the observation of the resonant frequencies with the following schedule:

- The master and slave recorders will be activated for low signal levels, which means that when a micro tremor occurs in the site the dynamic response of the two points are measured;
- Every month, a record of 10 minutes is performed in the two recorders in order to detect frequency shifts in the eigenfrequencies. This will allow to separate the influence of environmental conditions and to compare through time the consecutive dynamic responses before and after the occurrence of significant events;
- Seasonally, 10 minutes records in every hour and during one complete day will be performed to observe, again, the influence of environmental conditions in the dynamic response of the church.

All the events are acquired at 100 samples per second. Between April 21 and May 12, 2005, only two sets of 10 minutes programmed data records were acquired. The maximum acceleration value was record in the sensor A2 with a value equal to 8.5 mg and in the y direction. Table 2 presents the maximum acceleration values that occurred for each direction during the two events. The table also presents the relation between the maximum acceleration in the same direction for the same event. The maximum value is equal to 29.2 and occurs in the y direction. It is also possible to conclude that the values of the first record are higher than the second one. This could be justified by a higher wind speed acting in the structure during the first event. This indicates the need to install a sensor to measure the wind velocity and direction in order to compare it with the results.

TABLE 2: Maximum acceleration values [mg] for $t_1 = \text{April 26, 2005}$ (14:00h) and $t_2 = \text{May 12, 2005}$ (14:00h).

| | Sensor A1 (base) | | | Sensor A2 (base) | | | A2/A1 | | |
|-------|------------------|------|------|------------------|-------------|------|-------|-------------|------|
| | x | y | z | X | y | z | x | y | z |
| t_1 | 0.24 | 0.29 | 0.26 | 2.84 | 8.47 | 6.75 | 11.8 | 29.2 | 26.0 |
| t_2 | 0.14 | 0.14 | 0.18 | 0.28 | 0.42 | 0.87 | 2.0 | 3.0 | 4.8 |

For the same dates and direction y, Figure 15a shows the auto spectrum of the sensor A2, where the shifts between the two time records are very small and can be only perceptible for the frequencies peaks below 5 Hz. Detail analysis of this shifts are premature at this stage, because it is necessary to have more

data records and the values of temperature from the static system to evaluate the environmental changes in the dynamic response of the structure.

Figure 15b presents the coherence between the base and the nave sensor in the y direction. It is possible to observe small coherence values between the signals, with a maximum of 0.5 for frequencies below 5 Hz. These values can be justified by the distance between the two measured points, which can reduce the signal correlation, or by the fact that these events were programmed and they do not correspond to a site tremor.

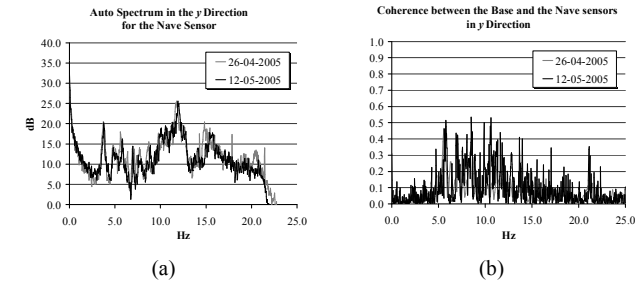


Fig. 15. Events comparison in y direction: (a) auto spectrum; (b) coherence values.

After the first results, the trigger levels were reconfigured in order to be able to record micro tremors. The acceleration levels for the sensor A1 (on the base) were adjusted to 0.5 mg in all directions and for the sensor A2 (on the main nave) to 10 mg in x direction and to 50 mg for the y and z directions. It is stressed that the relation between the triggers of sensor A2 and A1 is about 50 in the y and z directions in order to avoid records when the wind speed is significant. Semester reports should be performed for the dynamic monitoring plan and in two years another dynamic modal analysis will be made to compare the results with the identification presented here.

CONCLUSIONS AND FURTHER DEVELOPMENTS

Dating from the 16th century, the Monastery of Jerónimos is, probably, the crown asset of Portuguese architectural heritage. Aiming at the study of its structural safety and seismic resistance, preliminary studies included a numerical non-linear analysis of the main and transept naves. Given the cultural importance of the construction, the safety of the users, the seismic hazard and the accumulation of physical, chemical and mechanical damage, complementary NDT were proposed. In the present paper only the two last tasks of the proposed testing program were presented: the first dynamic modal identification analysis and the implementation of two monitoring systems; a static and a dynamic one.

The dynamic modal identification tests were carried out with output-only experimental techniques and eight mode shapes were assessed. Two methods for the dynamic parameter estimation were used and compared and the results with higher accuracy are the resonate frequencies. The mode shape vectors correspond to local modes governed by the behaviour of the slender columns.

The static monitoring system is composed by two tilt meters and six temperature sensors connected to a data logger. The dynamic monitoring system, composed of two strong motions recorders, is also installed and in operation since April 21, 2005. Three weeks of observation were enough to see small frequency shifts in the response spectra, but a detailed analysis of these shifts is premature, because it is necessary to have more data records and the values of temperature from the static system, in order to evaluate the environmental changes in the dynamic response of the structure. The health monitoring of the church will be based on the observations of the changes in the static and dynamic response, apart from the contribution of the environmental structural influences.

ACKNOWLEDGEMENTS

The authors gratefully acknowledge the support of the European-Indian Economic Cross Cultural Program, under contract ALA/95/23/2003/077-122, "Improving the Seismic Resistance of Cultural Heritage Buildings".

REFERENCES

- Brincker, R.; Zhang, L. and Andrensen, P., Modal identification from ambient responses using frequency domain decomposition, Proceedings of the 18th International Seminar on Modal Analysis, San Antonio, Texas, 7-10 February. 2000.
- Brincker, R.; Ventura, C. and Andersen, P., Damping estimation by frequency domain decomposition, Proceedings of IMAC XIX, the 19th International Modal Analysis Conference, Kissimmee, USA. 2001.
- Doebling, S.; Farrar C.; Prime, M.; Shevitz, D., Damage identification and health monitoring of structural and mechanical systems from changes in their vibration characteristics: a literature review, Los Alamos National Laboratory, NM. 1996.
- Ewins, D.J., Modal testing, theory, practice and application, Second Edition, Research Studies Press LTD, Baldock, Hertfordshire, England. 2000.
- Genin, S., Descriptive study of the vault in the Church of the Monastery of Santa Maria de Belém in Lisbon (in French), M.Sc. Thesis, Katholieke Universiteit Leuven, Belgium. 1995.
- Genin, S., The nave vault of the Hieronymites Monastery Church in Lisbon, Proceedings of Historical Constructions 2001, Eds. P. Lourenço and P. Roca, Universidade do Minho, Guimarães, pp. 293-302. 2001.
- Lourenço, P.B., Mourão, S., Safety assessment of Monastery of Jerónimos, Proceedings of Historical Constructions 2001, Eds. P. Lourenço and P. Roca, Universidade do Minho, Guimarães, pp. 697-706. 2001.
- Lourenço, P.B., Krakowiak, K.J., Stability assessment of the vaults from the Church of Monastery of Jerónimos (in Portuguese), Report 03-DEC/E-02, Universidade do Minho, Portugal. 2003.
- Maeck, J., Damage Assessment of Civil Engineering Structures by Vibration Monitoring, PhD Thesis, Katholieke Universiteit Leuven, Belgium. 2003.
- Mun, M., Study of the constitution of the vaults in the Church from the Monastery of Jerónimos using radar and complementary diagnosis methods (in Portuguese), Report 176/2002, Laboratório Nacional de Engenharia Civil, Lisbon, Portugal. 2002.
- Oliveira, M.M.P., Radar investigation of the Church of Jerónimos (in Portuguese), Report 177/2002, Laboratório Nacional de Engenharia Civil, Lisbon, Portugal. 2002.
- Peeters, B., System Identification and Damage Detection in Civil Engineering, PhD Thesis, Katholieke Universiteit Leuven, Belgium. 2000.
- Rodrigues, J., Identificação modal estocástica, métodos de análise e aplicações em estruturas de engenharia civil (in Portuguese), PhD Thesis, Engineering Faculty of University of Porto, Portugal. 2004.
- TNO Building and Construction Research, DIANA finite element analysis, User's Manual, Release 8.1. 2002.